

# Voxel-based dual-time $^{18}\text{F}$ -FDG parametric imaging for rectal cancer: differentiation of residual tumor from postchemoradiotherapy changes

Hongyoon Choi<sup>a</sup>, Hai-jeon Yoon<sup>a</sup>, Tae Sung Kim<sup>a</sup>, Jae Hwan Oh<sup>b</sup>,  
Dae Yong Kim<sup>b</sup> and Seok-ki Kim<sup>a</sup>

**Introduction**  $^{18}\text{F}$ -Fluorodeoxyglucose ( $^{18}\text{F}$ -FDG) PET/computed tomography (CT) has been used for evaluation of the response of rectal cancer to neoadjuvant chemoradiotherapy (CRT), but differentiating residual tumor from post-treatment changes remains a problem. We propose a voxel-based dual-time  $^{18}\text{F}$ -FDG PET parametric imaging technique for the evaluation of residual rectal cancer after CRT.

**Materials and methods** Eighty-six patients with locally advanced rectal cancer who underwent neoadjuvant CRT between March 2009 and February 2011 were selected retrospectively. Standard 60-min postinjection PET/CT scans followed by 90-min delayed images were coregistered by rigid-body transformation. A dual-time parametric image was generated, which divided delayed standardized uptake value (SUV) by 60-min SUV on a voxel-by-voxel basis. Maximum delayed-to-standard SUV ratios (DSR) measured on the parametric images as well as the percentage of SUV decrease from pre-CRT to post-CRT scans (pre/post-CRT response index) were obtained for each tumor and correlated with pathologic response classified by the Dworak tumor regression grade (TRG).

**Results** With respect to the false-positive lesions in the nine post-CRT patients with false-positive standard  $^{18}\text{F}$ -FDG scans in case groups who responded to therapy

(TRG 3 or 4 tumors), eight were undetectable on dual-time parametric images ( $P < 0.05$ ). The maximum DSR showed significantly higher accuracy for identification of tumor regression compared with the pre/post-CRT response index in receiver-operating characteristic analysis ( $P < 0.01$ ). With a 1.25 cutoff value for the maximum DSR, 85.0% sensitivity, 95.5% specificity, and 93.0% overall accuracy were obtained for identification of good response.

**Conclusion** A voxel-based dual-time parametric imaging technique for evaluation of post-CRT rectal cancer holds promise for differentiating residual tumor from treatment-related nonspecific  $^{18}\text{F}$ -FDG uptake. *Nucl Med Commun* 34:1166–1173 © 2013 Wolters Kluwer Health | Lippincott Williams & Wilkins.

Nuclear Medicine Communications 2013, 34:1166–1173

**Keywords:** dual-time  $^{18}\text{F}$ -FDG PET,  $^{18}\text{F}$ -FDG parametric image,  $^{18}\text{F}$ -FDG PET/CT, rectal cancer, tumor regression grade

<sup>a</sup>Department of Nuclear Medicine and <sup>b</sup>Center for Colorectal Cancer, National Cancer Center, Goyang, Korea

Correspondence to Seok-ki Kim, MD, Department of Nuclear Medicine, National Cancer Center, 111 Jungbalsan-ro, Ilsandong-gu, Goyang-si, Gyeonggi-do 410-769, Korea  
Tel: +82 31 920 1731; fax: +82 31 920 0179;  
e-mail: sskim@ncc.re.kr

Received 21 June 2013 Revised 8 August 2013 Accepted 28 August 2013

## Introduction

Neoadjuvant chemoradiotherapy (CRT) in patients with locally advanced rectal cancer (LARC, higher than stage T3 and/or clinical evidence of lymph node metastasis) has been recommended for reducing tumor size and stage, with the goal of increased resectability and improved chance of sphincter preservation [1–3]. Several imaging techniques have been used for staging LARC and for assessing response to neoadjuvant CRT. Recently,  $^{18}\text{F}$ -fluorodeoxyglucose ( $^{18}\text{F}$ -FDG) PET was reported to be beneficial for the evaluation of treatment response in several cancers, including LARC [4–6].

Although functional imaging with  $^{18}\text{F}$ -FDG PET is a useful technique for evaluating treatment response, it has

some limitations. Increased  $^{18}\text{F}$ -FDG uptake is seen in inflammatory conditions [7]. Fibrosis or edema following irradiation can also be  $^{18}\text{F}$ -FDG-avid [8–11].

Dual-time  $^{18}\text{F}$ -FDG PET has been reported to improve diagnostic accuracy for several cancers [12,13]. This is based on the different pattern of  $^{18}\text{F}$ -FDG uptake in malignant tumors, which display slowly increasing  $^{18}\text{F}$ -FDG uptake, whereas benign lesions, including inflammation, show an earlier peak and then a decline. Recently, Prieto *et al.* [14] suggested the feasibility of voxel-based dual-time  $^{18}\text{F}$ -FDG PET images for brain tumors and showed that parametric images improved sensitivity for tumor identification.

We investigated voxel-based dual-time  $^{18}\text{F}$ -FDG PET parametric imaging in the evaluation for residual tumor after CRT in rectal cancer. We previously introduced volume-of-interest (VOI)-based quantitative analysis for

Supplemental digital content is available for this article. Direct URL citations appear in the printed text and are provided in the HTML and PDF versions of this article on the journal's website ([www.nuclearmedicinecomm.com](http://www.nuclearmedicinecomm.com)).

dual-time  $^{18}\text{F}$ -FDG uptake [15]. In this study, for an image-based CRT response evaluation, we developed dual-time parametric imaging, which can provide anatomical information as well as physiological parameters. As a feasibility study of the dual-time parametric imaging for post-CRT LARC, we performed visual analysis and measured the parameters quantitatively to differentiate residual viable tumor from post-CRT changes.

## Materials and methods

### Patients and clinical factors

From March 2009 to February 2011, patients with LARC who underwent neoadjuvant CRT were selected retrospectively. Among them, 86 patients underwent  $^{18}\text{F}$ -FDG PET/CT scans, first as a staging workup and then for response evaluation after neoadjuvant CRT. This study represents a new image-based version of a previous investigation on the diagnostic accuracy of dual-time  $^{18}\text{F}$ -FDG PET in post-CRT patients [15]. The present study included 61 patients who had been previously enrolled. To be eligible the patients had to have undergone two  $^{18}\text{F}$ -FDG PET/CT scans, one for initial staging and the other after CRT for post-treatment evaluation. Table 1 summarizes the clinical characteristics of our study. All patients had biopsy-proven LARC. This study was approved by the Institutional Review Board.

### $^{18}\text{F}$ -FDG PET/CT scans

According to the protocol of our previous study [15],  $^{18}\text{F}$ -FDG PET/CT was performed before and after CRT. Patients with blood glucose levels lower than 6.67 mmol/l (120 mg/dl) were injected intravenously with 7.4 MBq/kg of  $^{18}\text{F}$ -FDG after fasting for at least 6 h. According to the standard protocol of our institute, PET/CT scans should commence 60 min after injection. Three dedicated PET/CT scanners were used (Biograph LSO; Siemens Medical Systems, Erlangen, Germany; and Discovery LS and Discovery STE; General Electric Medical Systems, Milwaukee, Wisconsin, USA). Post-CRT PET/CT scans were performed using a dual-time-point protocol, which included the standard whole-body acquisition at 60 min (range 51–94 min) and a delayed acquisition of the lower abdomen and pelvis at 90 min (range 79–130 min) after injection. Both pre-CRT and

post-CRT PET scans were performed using the same scanner for each patient. PET images were reconstructed using an iterative algorithm (ordered-subset expectation maximization) with an image matrix size of  $128 \times 128$ .

### Image processing

To correct positioning artifacts, post-CRT standard and delayed images were coregistered using a statistical parametric mapping software package (SPM2; University College London, London, UK). More specifically, rigid-body transformation was carried out using three translations and three rotation parameters. All transformed images were visually confirmed. Each image was scaled and quantitatively displayed by the standardized uptake value (SUV). A spherical VOI was placed around abnormalities with increased  $^{18}\text{F}$ -FDG uptake on images, and the delayed SUV was divided by standard SUV on a voxel basis. A dual-time parametric image was created from each post-CRT image, with a delayed-to-standard SUV ratio (DSR) map (Fig. 1).

### PET/CT-based response assessment

The patients with undetectable  $^{18}\text{F}$ -FDG uptake in post-CRT images were regarded as good responders. In patients with detectable post-CRT activity, tumor response was first evaluated using a pre/post-CRT response index (RI) by using manually drawn VOIs to determine the maximum SUV ratio of tumor sites between pre-CRT and post-CRT standard PET/CT scans. A VOI-based delayed-to-standard index (DI), the maximum SUV ratio between delayed and 60-min post-CRT PET/CT scans, was also computed for each volume pair. Tumor response evaluation using delayed-to-standard parametric mapping was also performed. When there was visible increased uptake on post-CRT images, the maximum DSR was obtained. Visual analysis was also carried out when lesions with increased DSRs were identifiable on the parametric map. Patients with visually identified foci on the DSR parametric maps were regarded as nonresponders, assuming that continuously increasing  $^{18}\text{F}$ -FDG uptake would represent residual viable tumor, whereas patients with undetectable activity on DSR maps were considered responders (Fig. 2).

SUV measurement was performed at a workstation with AW 4.3 software (General Electric Medical Systems). DSR parametric maps were visually evaluated using PET with combined CT, and pre-CRT and post-CRT PET/CT scans were compared slice by slice.

### Pathological response assessment

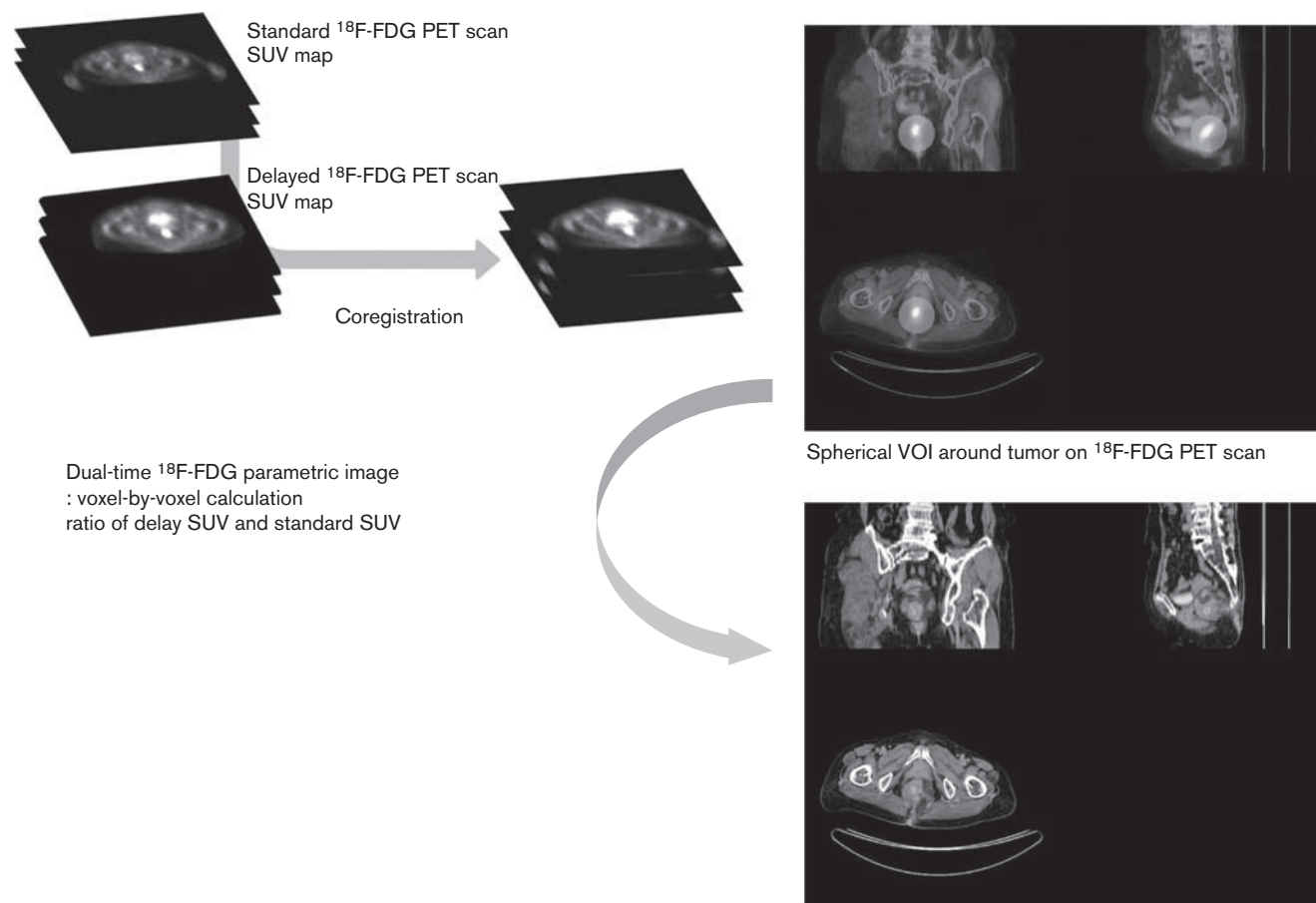
Patients underwent surgery after completing CRT. The surgical specimens were evaluated by experienced pathologists. Tumor regression grade (TRG) was classified into one of five categories according to the Dworak tumor grading system [9]: TRG 4, total regression; TRG 3, near-total regression; TRG 2, moderate regression; TRG 1, minimal regression; and TRG 0, no regression. Tumors

**Table 1** Clinical characteristics of the patients

	<i>N</i> =86
Age (years)	59.2 (range 30–85)
Sex [ <i>n</i> (%)]	
Male	61 (70.9)
Female	25 (29.1)
T-stage (initial, clinical stage)	T3 77 (89.5%) T4 9 (10.5%)
N-stage (initial, clinical stage)	N0 10 (11.6%) N1 76 (88.4%)
Chemotherapy regimen	FL 47 (54.7%) UFT + LV 34 (39.5%) Xeloda 5 (5.8%)

FL, fluorouracil, leucovorin; LV, leucovorin; UFT, Tegafur-uracil.

Fig. 1



Schematic workflow for dual-time parametric image reconstruction. Delayed and standard PET images were scaled to standardized uptake value (SUV) and coregistered. A spherical volume-of-interest (VOI) was drawn around a focus detectable on the postchemoradiotherapy  $^{18}\text{F}$ -FDG PET/CT scan and the delayed-to-standard SUV ratio was calculated on a voxel basis. CT, computed tomography;  $^{18}\text{F}$ -FDG,  $^{18}\text{F}$ -fluorodeoxyglucose.

with TRG 3 and TRG 4 were included in the responders group, whereas tumors with TRG 0, TRG 1, and TRG 2 were included in the nonresponders group.

### Statistical analysis

Pearson's  $\chi^2$ -test was performed to analyze the categorical variables, including clinical characteristics. Receiver-operating characteristics (ROC) curves were drawn for the pre/post-CRT RI, for DI and for maximum DSR for the evaluation of pathologic response. Sensitivity, specificity, and accuracy were calculated for each test variable using the optimal threshold value.  $P$  values less than 0.05 were considered significant. Statistical analyses were performed using SPSS software (version 18; SPSS Inc., Chicago, Illinois, USA).

## Results

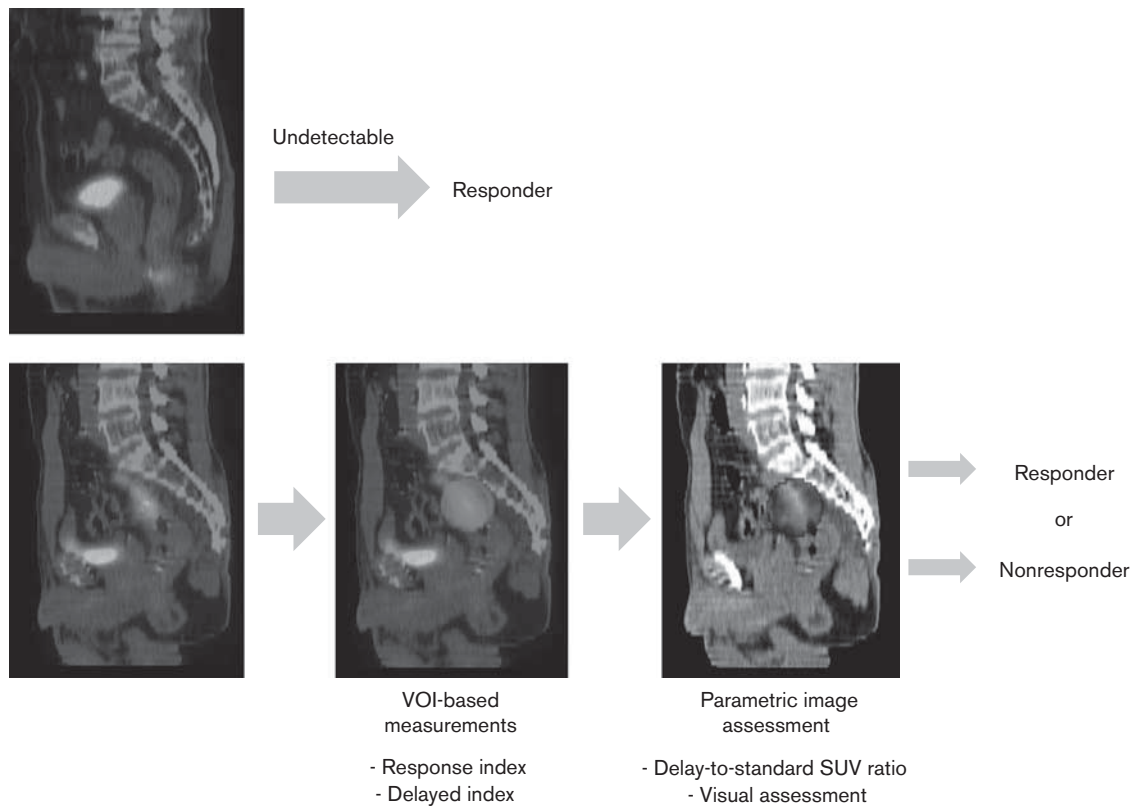
### Dual-time parametric maps for post-CRT tumors

Seventy-two patients showed detectable  $^{18}\text{F}$ -FDG uptake in lesions on post-CRT PET/CT scans. Nine of them were classified by pathological analysis as total or near-

total regression (TRG 3 and 4). These nine patients were regarded as showing false-positive  $^{18}\text{F}$ -FDG uptake on standard scans. There was no definite discernible lesion on the dual-time parametric map in eight cases ( $P < 0.05$ ,  $\chi^2 = 5.44$ ).

Representative cases from the responding and nonresponding groups are shown in Fig. 3. As shown in Fig. 3a and b, the post-CRT PET/CT scan shows an ill-defined lesion with mildly increased  $^{18}\text{F}$ -FDG uptake; however, the voxel-based dual-time parametric image shows a high DSR in the lesion, which was confirmed as TRG 2, moderate regression. Figure 3c and d shows an example of increased  $^{18}\text{F}$ -FDG uptake due to post-CRT inflammation. Intense  $^{18}\text{F}$ -FDG uptake at the tumor site was found on the post-CRT PET/CT scan; however, the dual-time parametric map showed no increased DSR in the same lesion. It was confirmed as TRG 4, total regression. More representative cases of each TRG are shown in Supplementary Fig. 1 (Supplemental digital content 1, <http://links.lww.com/NMC/A16>).

Fig. 2



Workflow for PET/CT-based response assessment. Patients with undetectable  $^{18}\text{F}$ -FDG uptake in post-CRT images were regarded as responders. CRT response was evaluated using VOI-based parameters (response index and delayed-to-standard index) and parametric image-based parameter (delayed-to-standard SUV ratio). Visual analysis was also performed on the parametric map. CRT, chemoradiotherapy; CT, computed tomography;  $^{18}\text{F}$ -FDG,  $^{18}\text{F}$ -fluorodeoxyglucose; SUV, standardized uptake value; VOI, volume-of-interest.

### $^{18}\text{F}$ -FDG PET parameters and prediction of response to treatment

The results of the ROC analysis of the RI, DI, and maximum DSR in relation to pathological response grade are shown in Fig. 4. DI values were obtained from the VOI-based maximum SUV ratio between standard and delayed scans, whereas maximum DSRs are the SUV ratios on a voxel-based parametric image. ROC analysis identified maximum DSR as the best indicator of response to CRT. Area under the curve (AUC) was significantly higher in maximum DSR compared with the pre/post-CRT RI. The analysis also suggested that DSR is a better indicator of CRT response compared with the VOI-based dual-phase index, although not to a statistically significant extent (AUC: 0.923 for DSR, 0.889 for DI, 0.758 for RI;  $P < 0.01$  for DSR vs. RI,  $P = 0.44$  for DSR vs. DI) (Fig. 4a).

We compared maximum DSR, DI, and RI, except for 14 cases with undetectable  $^{18}\text{F}$ -FDG uptake in post-CRT PET/CT scans. The DSR and DI showed significantly higher AUCs compared with RI. There was no significant difference between DSR and DI (AUC: 0.902 for DSR,

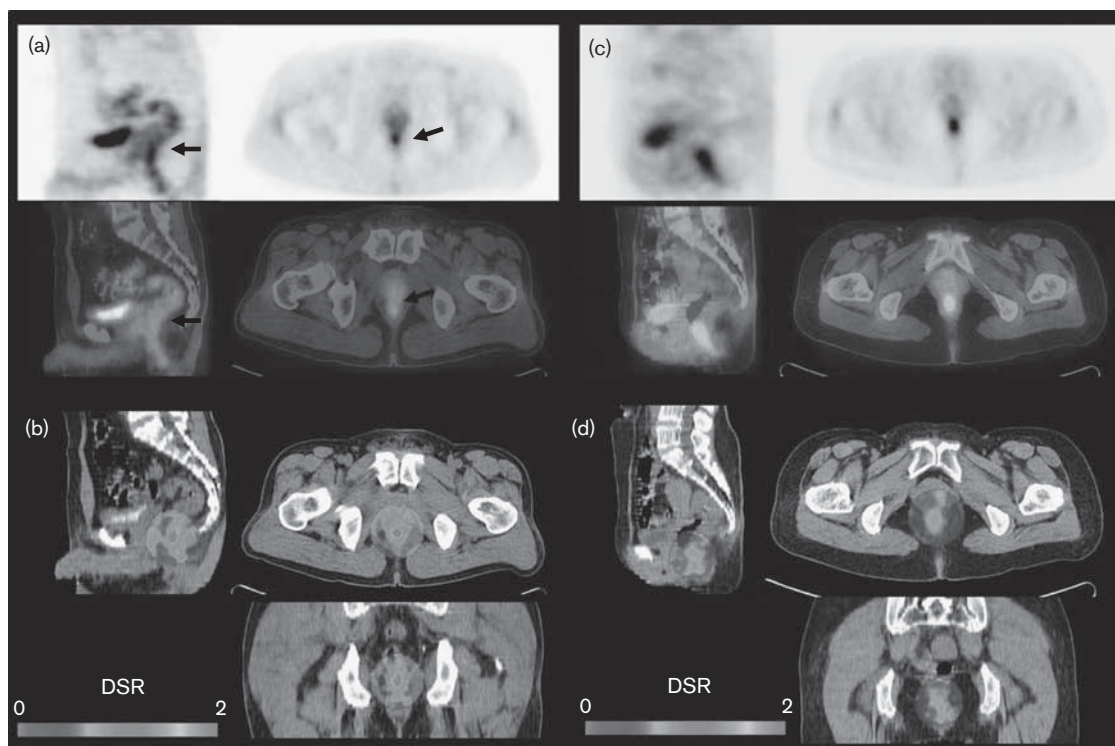
0.848 for DI, 0.517 for RI;  $P < 0.001$  for DSR vs. RI,  $P < 0.05$  for DI vs. RI,  $P = 0.57$  for DSR vs. DI) (Fig. 4b).

The sensitivity, specificity, and accuracy of PET/CT parameters for prediction of response to CRT are summarized in Table 2. In brief, with a 1.25 cutoff value for the maximum DSR, 85.0% sensitivity, 95.5% specificity, and 93.0% overall accuracy were obtained for the responding group, which was higher than the DI and RI. Compared with DI-based response evaluation, maximum DSR improved on positive predictive value (75 and 85%, respectively) and negative predictive value (90.9 and 95.5%, respectively). A graphical summary of comparison between the two methods is shown in Fig. 5.

### Discussion

In the current study, we generated dual-time parametric images of  $^{18}\text{F}$ -FDG PET/CT for evaluation for residual tumor versus inflammation after neoadjuvant CRT on a voxel basis instead of using VOIs. We evaluated maximum DSR for CRT response obtained from the parametric images, and visual assessment was also performed. As a result, most foci with false-positive  $^{18}\text{F}$ -FDG uptake

Fig. 3



Two representative cases of post-CRT dual-time parametric images: (a, b) nonresponding case and (c, d) responding case. (a) The post-CRT tumor shows increased SUV in the  $^{18}\text{F}$ -FDG PET/CT image (arrow,  $\text{SUV}_{\text{max}}$  4.1). (b) The dual-time parametric image shows focal lesion clearly with increased delayed-to-standard SUV ratio (maximum DSR, 2.31). The post-CRT  $^{18}\text{F}$ -FDG PET/CT image shows a relatively indistinctive margin and larger extent compared with the dual-time parametric map. The surgical specimen revealed Dworak regression grade 2, regarded as nonresponder. (c) The post-CRT PET/CT scan shows increased  $^{18}\text{F}$ -FDG uptake ( $\text{SUV}_{\text{max}}$  5.9). (d) The lesion identified on the  $^{18}\text{F}$ -FDG PET/CT scan shows a low DSR in the dual-time parametric image (maximum DSR, 1.23). The surgical specimen revealed Dworak regression grade 4, total regression. CRT, chemoradiotherapy; CT, computed tomography;  $^{18}\text{F}$ -FDG,  $^{18}\text{F}$ -fluorodeoxyglucose;  $\text{SUV}_{\text{max}}$ , maximum standardized uptake value; VOI, volume-of-interest.

exhibited no detectable foci on DSR parametric maps. Maximum DSR showed higher diagnostic accuracy than did the RI obtained from pre-CRT and post-CRT PET/CT scans.

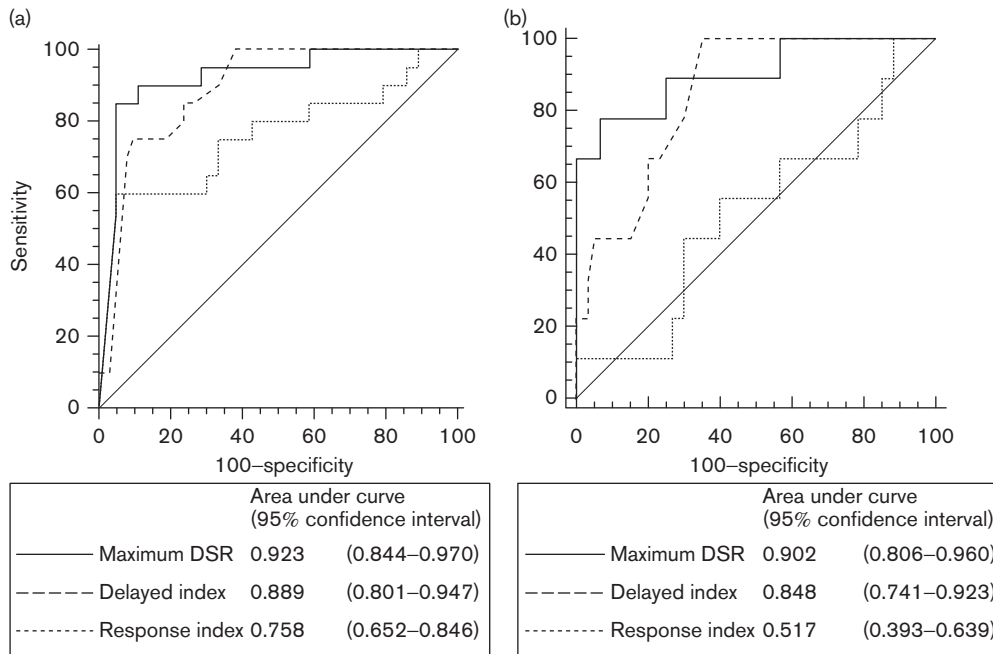
Recent studies have reported that changes in  $^{18}\text{F}$ -FDG uptake before and after CRT could differentiate responders from nonresponders and predict the patient's outcome [16,17]. However,  $^{18}\text{F}$ -FDG uptake has been reported to be nonspecific for malignant tumors, particularly in post-CRT rectal cancers, because of radiation-induced inflammation and physiological bowel uptake [10,11,18]. Because preoperative residual tumor evaluation is important for performing minimally invasive surgery such as sphincter preservation, an accurate noninvasive diagnostic image-based approach has been sought.

To our knowledge, this study is the first to evaluate voxel-based dual-time parametric mapping for CRT response. The difference in  $^{18}\text{F}$ -FDG uptake between standard and delayed post-treatment scans was evaluated in several cancers to differentiate malignancy from inflammation [13]. Voxel-based analysis is an image-based approach, which uses anatomical information, unlike VOI-based

analysis. Thus, this approach enables calculation of the real increase in  $^{18}\text{F}$ -FDG uptake in delayed scans, as SUV is measured in the same voxel. As reported in our previous study [15], dual-time  $^{18}\text{F}$ -FDG PET/CT exhibited better accuracy in diagnosing tumor response compared with the changes between pre-CRT and post-CRT  $^{18}\text{F}$ -FDG uptake. We further investigated voxel-based parametric imaging instead of VOIs. Our results trended toward improved diagnostic accuracy, although statistical significance was not reached.

Compared with the VOI-based method, our parametric image-based approach provides anatomical information, which is important for assessing for residual tumor. In the current study, parametric imaging and the VOI-based DI showed no significant difference between the AUC of maximum DSR. However, anatomical information using parametric images may identify a culprit lesion in post-CRT  $^{18}\text{F}$ -FDG PET/CT images. Because inflammatory cells around tumors contribute to the  $^{18}\text{F}$ -FDG uptake, anatomical differentiation between viable tumor and inflammation on post-CRT scans is difficult [10,19]. As shown in Fig. 3, a residual tumor lesion was more clearly identified on the

Fig. 4



Receiver-operating characteristic curves of delayed-to-standard SUV ratio (DSR), volume-of-interest-based dual-phase index (DI) and pre/post-CRT response index (RI). (a) DSR had a significantly higher AUC compared with RI for all cases ( $P < 0.01$ ). (b) Excluding the cases with undetectable  $^{18}\text{F}$ -FDG uptake in post-CRT scans, DSR and DI showed significantly higher AUCs compared with RI ( $P < 0.001$  for DSR vs. RI;  $P < 0.05$  for DI vs. RI). AUC, area under the curve; CRT, chemoradiotherapy;  $^{18}\text{F}$ -FDG,  $^{18}\text{F}$ -fluorodeoxyglucose.

Table 2 Sensitivity, specificity, and accuracy of response to treatment

	Visual analysis with DSR map	Maximum DSR <sup>a</sup>	VOI-based delayed-to-standard index (DI) <sup>b</sup>	Response index <sup>c</sup>
Sensitivity	70.0 (50.8–82.3)	85.0 (66.9–94.6)	75.0 (55.2–88.4)	60.0 (41.5–70.7)
Specificity	93.9 (88.1–97.7)	95.5 (90.0–98.4)	90.9 (84.9–95.0)	95.2 (89.3–98.6)
Accuracy	88.4 (79.4–94.1)	93.0 (84.6–97.5)	87.2 (78.0–93.5)	86.7 (77.8–91.9)

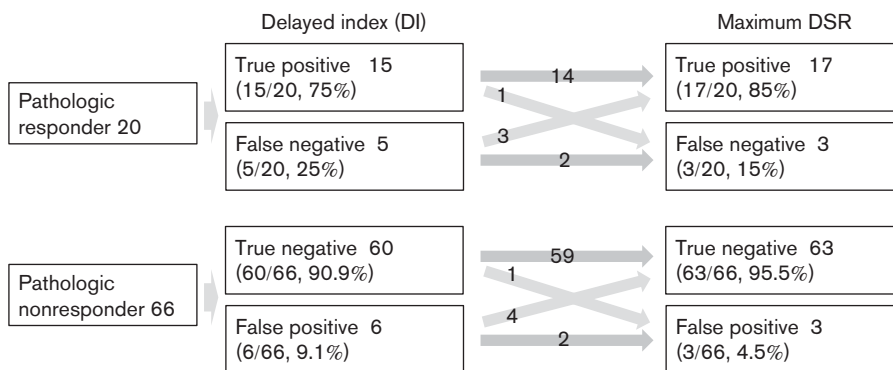
CRT, chemoradiotherapy; DSR, delayed-to-standard SUV ratios; VOI, volume-of-interest.

<sup>a</sup>DSR  $\leq 1.253$  for responders.

<sup>b</sup>VOI-based dual-phase index  $\leq 0.02$  for responders.

<sup>c</sup>Pre/post-CRT response index  $> 84.89$  for responders.

Fig. 5



A comparison between the two methods for response evaluation: volume-of-interest-based delayed-to-standard index (DI) and maximum delayed-to-standard SUV ratio (DSR) on the dual-time parametric image.

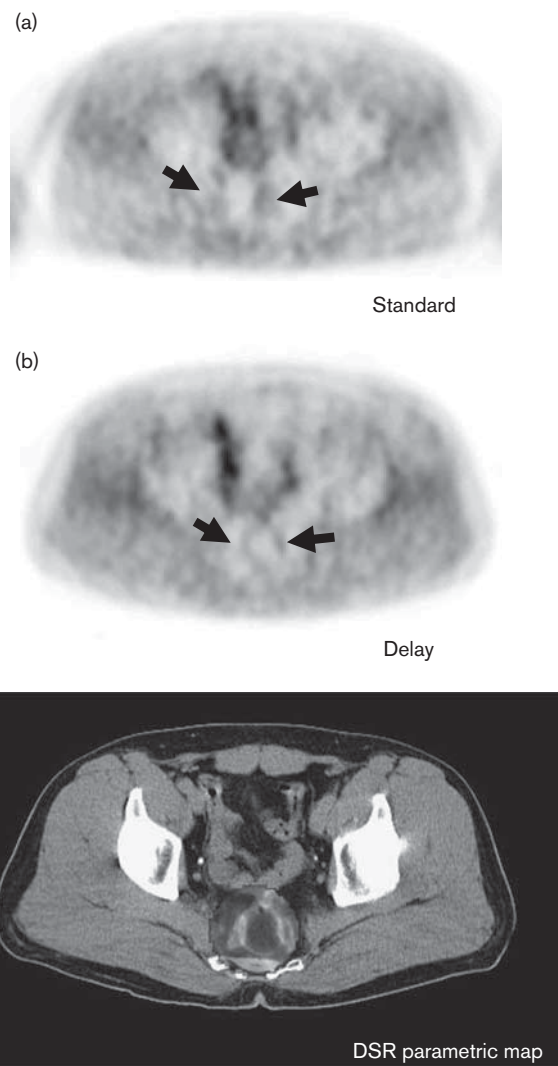
parametric image than on the post-CRT PET/CT scan. Our approach may detect intratumoral heterogeneous features of malignancy because of preserved anatomical information, unlike representative descriptive parameters such as RI and VOI-based DI. More importantly, manually drawn VOI-based maximum SUVs on standard and delayed scans cannot always be obtained from the same voxel [14]. Of note, parametric imaging would be helpful for measuring residual tumor extent, although further study regarding the correlation between parametric images and pathological findings is needed.

We used rigid-body coregistration of standard and delayed PET/CT scans to minimize the distortion of images. Because coregistration between standard and delayed scans is not perfect, a few areas on the parametric images appeared to show high-signal artifacts in parametric maps owing to misregistration or bowel peristalsis (Fig. 6). Therefore, dual-time parametric maps were only applied to tumors that showed visually detectable  $^{18}\text{F}$ -FDG uptake in post-CRT PET/CT scans using spherical VOIs around the tumors to minimize the noise effect. Moreover, each of the scans was visually evaluated to find bowel peristalsis or misregistration, and maximum DSR values were derived only in the known tumor area. The misregistration artifact was also one of the limitations to developing parametric response images using  $^{18}\text{F}$ -FDG PET/CT, a recently proposed technique for image-based treatment response monitoring [20]. Although standard and delayed scans conceivably have fewer changes between them compared with pre-CRT and post-CRT scans, further investigation of better registration methods and dual-time acquisition protocols is warranted to reduce misregistration.

The maximum DSR was calculated to assess quantitatively whether visually detectable lesions in post-CRT scans represented residual viable tumor or benign inflammatory changes. Malignancy has a feature of slowly increasing  $^{18}\text{F}$ -FDG uptake [13]. Malignant lesions generally have a higher DSR compared with inflammatory lesions. A limitation of this study is the unknown clinical or biological significance of the maximum DSR; the degree of increased  $^{18}\text{F}$ -FDG uptake in the delayed phase does not necessarily reflect disease severity, whereas the maximum SUV parallels the metabolic activity of tumors. Furthermore, in this study, time differences between standard and delayed scans were not perfectly controlled, which could affect the maximum DSR value. In this context, we performed visual analysis to detect tumor lesions on the parametric images. The diagnostic accuracy was also higher than that of RI or DI, although statistical significance was not reached.

The design of this study was retrospective and selection bias may have existed. Although our inclusion criteria excluded no patients to minimize bias, and we obtained consistent results, a prospective investigation is warranted. The PET/CT study protocol for establishing the best dual-time parametric imaging technique with

**Fig. 6**



A standard  $^{18}\text{F}$ -FDG PET/CT scan (a) and a delayed  $^{18}\text{F}$ -FDG PET/CT scan (b) were misaligned probably because of bowel peristalsis, and an artifact of marginal high signal was found on the dual-time parametric image (c). CT, computed tomography;  $^{18}\text{F}$ -FDG,  $^{18}\text{F}$ -fluorodeoxyglucose.

respect to scan time and registration strategies has not been optimized yet. As a feasibility study, we propose dual-time parametric image-based evaluation for tumor regression; however, tumor delineation on parametric images, comparing the parametric images and surgical specimens, has not been studied. In the future, our proposed approach may be useful for evaluating the anatomical extent of residual tumors after neoadjuvant CRT for further therapeutic planning.

## Conclusion

Dual-time parametric imaging for differentiating residual tumor from inflammation after neoadjuvant CRT in rectal

cancer is a promising method. Although further studies on tumor delineation and accurate registration methods are needed, our new image-based approach provides visual depiction of residual tumor, as well as differentiation from false-positive  $^{18}\text{F}$ -FDG uptake in inflammation.

## Acknowledgements

This research was supported by the Bio & Medical Technology Development Program of the National Research Foundation (NRF) funded by the Korean government (MEST) (2012-0005987).

## Conflicts of interest

There are no conflicts of interest.

## References

- Kapiteijn E, Marijnen CA, Nagtegaal ID, Putter H, Steup WH, Wiggers T, *et al.* Preoperative radiotherapy combined with total mesorectal excision for resectable rectal cancer. *N Engl J Med* 2001; **345**:638–646.
- De Paoli A, Chiara S, Luppi G, Friso ML, Beretta GD, Del Prete S, *et al.* Capecitabine in combination with preoperative radiation therapy in locally advanced, resectable, rectal cancer: a multicentric phase II study. *Ann Oncol* 2006; **17**:246–251.
- Peeters KC, Marijnen CA, Nagtegaal ID, Kranenbarg EK, Putter H, Wiggers T, *et al.* The TME trial after a median follow-up of 6 years: increased local control but no survival benefit in irradiated patients with resectable rectal carcinoma. *Ann Surg* 2007; **246**:693–701.
- Beets-Tan RG, Beets GL, Vliegen RF, Kessels AG, Van Boven H, De Bruine A, *et al.* Accuracy of magnetic resonance imaging in prediction of tumour-free resection margin in rectal cancer surgery. *Lancet* 2001; **357**:497–504.
- Cascini GL, Avallone A, Delrio P, Guida C, Tatangelo F, Marone P, *et al.*  $^{18}\text{F}$ -FDG PET is an early predictor of pathologic tumor response to preoperative radiochemotherapy in locally advanced rectal cancer. *J Nucl Med* 2006; **47**:1241–1248.
- Capirci C, Rampin L, Erba PA, Galeotti F, Crepaldi G, Banti E, *et al.* Sequential FDG-PET/CT reliably predicts response of locally advanced rectal cancer to neo-adjuvant chemo-radiation therapy. *Eur J Nucl Med Mol Imaging* 2007; **34**:1583–1593.
- Zhuang H, Alavi A.  $^{18}\text{F}$ -Fluorodeoxyglucose positron emission tomographic imaging in the detection and monitoring of infection and inflammation. *Semin Nucl Med* 2002; **32**:47–59.
- Vecchio FM, Valentini V, Minsky BD, Padula GD, Venkatraman ES, Balducci M, *et al.* The relationship of pathologic tumor regression grade (TRG) and outcomes after preoperative therapy in rectal cancer. *Int J Radiat Oncol Biol Phys* 2005; **62**:752–760.
- Dworak O, Keilholz L, Hoffmann A. Pathological features of rectal cancer after preoperative radiochemotherapy. *Int J Colorectal Dis* 1997; **12**:19–23.
- Haberkorn U, Strauss LG, Dimitrakopoulou A, Engenhart R, Oberdorfer F, Ostertag H, *et al.* PET studies of fluorodeoxyglucose metabolism in patients with recurrent colorectal tumors receiving radiotherapy. *J Nucl Med* 1991; **32**:1485–1490.
- Janssen MH, Ollers MC, Riedl RG, van den Bogaard J, Buijsen J, van Stiphout RG, *et al.* Accurate prediction of pathological rectal tumor response after two weeks of preoperative radiochemotherapy using  $^{18}\text{F}$ -fluorodeoxyglucose-positron emission tomography-computed tomography imaging. *Int J Radiat Oncol Biol Phys* 2010; **77**:392–399.
- Basu S, Alavi A. Partial volume correction of standardized uptake values and the dual time point in FDG-PET imaging: should these be routinely employed in assessing patients with cancer? *Eur J Nucl Med Mol Imaging* 2007; **34**:1527–1529.
- Schillaci O. Use of dual-point fluorodeoxyglucose imaging to enhance sensitivity and specificity. *Semin Nucl Med* 2012; **42**:267–280.
- Prieto E, Marti-Ciement JM, Dominguez-Prado I, Garrastachu P, Diez-Valle R, Tejada S, *et al.* Voxel-based analysis of dual-time-point  $^{18}\text{F}$ -FDG PET images for brain tumor identification and delineation. *J Nucl Med* 2011; **52**:865–872.
- Yoon HJ, Kim SK, Kim TS, Im HJ, Lee ES, Kim HC, *et al.* New application of dual time point  $^{18}\text{F}$ -FDG PET/CT in the evaluation of neoadjuvant chemoradiation response of locally advanced rectal cancer. *Clin Nucl Med* 2013; **38**:7–12.
- Avallone A, Aloj L, Caraco C, Delrio P, Pecori B, Tatangelo F, *et al.* Early FDG PET response assessment of preoperative radiochemotherapy in locally advanced rectal cancer: correlation with long-term outcome. *Eur J Nucl Med Mol Imaging* 2012; **39**:1848–1857.
- Yeung JM, Kalf V, Hicks RJ, Drummond E, Link E, Taouk Y, *et al.* Metabolic response of rectal cancer assessed by  $^{18}\text{F}$ -FDG PET following chemoradiotherapy is prognostic for patient outcome. *Dis Colon Rectum* 2011; **54**:518–525.
- Rosenberg R, Herrmann K, Gertler R, Kunzli B, Essler M, Lordick F, *et al.* The predictive value of metabolic response to preoperative radiochemotherapy in locally advanced rectal cancer measured by PET/CT. *Int J Colorectal Dis* 2009; **24**:191–200.
- Kubota R, Yamada S, Kubota K, Ishiwata K, Tamahashi N, Ido T. Intratumoral distribution of fluorine-18-fluorodeoxyglucose in vivo: high accumulation in macrophages and granulation tissues studied by microautoradiography. *J Nucl Med* 1992; **33**:1972–1980.
- Necib H, Garcia C, Wagner A, Vanderlinden B, Emonts P, Hendlisz A, *et al.* Detection and characterization of tumor changes in  $^{18}\text{F}$ -FDG PET patient monitoring using parametric imaging. *J Nucl Med* 2011; **52**:354–361.